



# In vivo 3'-to-5' exoribonuclease targetomes of *Streptococcus pyogenes*

Anne-Laure Lécrivain<sup>a,b,c,1</sup>, Anaïs Le Rhun<sup>a,b,1</sup>, Thibaud T. Renault<sup>a,b,d</sup>, Rina Ahmed-Begrich<sup>a,b</sup>, Karin Hahnke<sup>a,b</sup>, and Emmanuelle Charpentier<sup>a,b,d,2</sup>

<sup>a</sup>Max Planck Unit for the Science of Pathogens, D-10117 Berlin, Germany; <sup>b</sup>Department of Regulation in Infection Biology, Max Planck Institute for Infection Biology, D-10117 Berlin, Germany; <sup>c</sup>Laboratory for Molecular Infection Medicine Sweden, Umeå Centre for Microbial Research, Department of Molecular Biology, Umeå University, S-90187 Umeå, Sweden; and <sup>d</sup>Institute for Biology, Humboldt University, D-10115 Berlin, Germany

Edited by Gisela Storz, National Institute of Child Health and Human Development, Bethesda, MD, and approved October 2, 2018 (received for review June 5, 2018)

mRNA decay plays an essential role in the control of gene expression in bacteria. Exoribonucleases (exoRNases), which trim transcripts starting from the 5' or 3' end, are particularly important to fully degrade unwanted transcripts and renew the pool of nucleotides available in the cell. While recent techniques have allowed genome-wide identification of ribonuclease (RNase) targets in bacteria in vivo, none of the 3'-to-5' exoRNase targetomes (i.e., global processing sites) have been studied so far. Here, we report the targetomes of YhaM, polynucleotide phosphorylase (PNPase), and RNase R of the human pathogen *Streptococcus pyogenes*. We determined that YhaM is an unspecific enzyme that trims a few nucleotides and targets the majority of transcript ends, generated either by transcription termination or by endonucleolytic activity. The molecular determinants for YhaM-limited processivity are yet to be deciphered. We showed that PNPase clears the cell from mRNA decay fragments produced by endoribonucleases (endoRNases) and is the major 3'-to-5' exoRNase for RNA turnover in *S. pyogenes*. In particular, PNPase is responsible for the degradation of regulatory elements from 5' untranslated regions. However, we observed little RNase R activity in standard culture conditions. Overall, our study sheds light on the very distinct features of *S. pyogenes* 3'-to-5' exoRNases.

3'-to-5' exoRNase | 5'-end sequencing | 3'-end sequencing | *Streptococcus pyogenes* | RNA degradation

The adaptation of bacteria to new environments requires rapid control of gene expression in response to external changes. Ribonucleases (RNases) participate in this regulatory process by stabilizing or degrading specific subsets of transcripts.

Although the set of RNases, and therefore the RNA degradation pathways, varies among bacterial species, a general model for RNA decay based on studies in *Escherichia coli* and *Bacillus subtilis* has been commonly accepted (1, 2). In this model, an initial step of degradation is performed by an endoribonuclease (endoRNase) that makes the transcripts accessible to other enzymes. Exoribonucleases (exoRNases) further process these transcripts into short oligoRNAs, which are then fully degraded by oligoRNase/nanoRNases.

Among the set of 3'-to-5' exoRNases, the main enzymes responsible for RNA degradation in bacteria are polynucleotide phosphorylase (PNPase), RNase R, and RNase II (the latter is not present in Gram-positive bacteria) (3). In their absence, other 3'-to-5' exoRNases (e.g., RNase PH, Gram-positive specific enzyme YhaM) can take over this process, albeit in a more limited fashion (4). The 3'-to-5' exoRNases possess distinct features that define their individual role in RNA decay. PNPase and RNase R require an unstructured tail of at least 7–10 nt to bind and degrade transcripts (5, 6). Only RNase R possesses an intrinsic unwinding activity that allows progressing through strong RNA structures (7, 8), although PNPase can process these structures by associating with an RNA helicase (9, 10).

The features attributed to 3'-to-5' exoRNases have been generalized from investigations in a limited number of bacteria. For example, the in vivo exoribonucleolytic activity of YhaM has been exclusively examined in *B. subtilis* (11, 12). It has become evident that RNases from diverse bacterial species have evolved specific characteristics, as illustrated by the observed variations of PNPase ortholog activities (13), therefore underlining the importance of studying RNases in various bacteria.

In this regard, the knowledge of RNase activities in the Gram-positive human pathogen *Streptococcus pyogenes* remains limited. We previously developed a method to identify in vivo processing sites of endoRNase III by RNA sequencing (14). We compared the abundance of 5' and 3' ends between wild type (WT) and  $\Delta$ mase at each genomic position with the following parameters: (i) the “expression” parameter ensures that the RNA is expressed at this position in WT and  $\Delta$ mase, and that there are a sufficient number of transcripts ending at this position in the WT; (ii) the “proportion of ends” parameter estimates the proportion of transcripts ending at one position over the total

## Significance

To cope with harsh environments and cause infection, bacteria need to constantly adjust gene expression. Ribonucleases (RNases) control the abundance of regulatory and protein-coding RNA through degradation and maturation. The current characterization of 3'-to-5' exoribonucleases (exoRNases), processing RNAs from their 3' end, is solely based on the description of a limited number of targets processed by these RNases. Here, we characterized bacterial 3'-to-5' exoRNase targetomes. We show that YhaM, polynucleotide phosphorylase (PNPase), and RNase R have exoribonucleolytic activities in the human pathogen *Streptococcus pyogenes*. We demonstrate that PNPase is the main 3'-to-5' exoRNase participating in RNA decay, we show that RNase R has a limited processing activity, and we describe an intriguing RNA processing behavior for YhaM.

Author contributions: A.-L.L., A.L.R., and E.C. designed research; A.-L.L., A.L.R., and K.H. performed research; A.-L.L., A.L.R., T.T.R., and R.A.-B. contributed new reagents/analytic tools; A.-L.L., A.L.R., and T.T.R. analyzed data; E.C. oversaw the project; and A.-L.L., A.L.R., T.T.R., and E.C. wrote the paper.

The authors declare no conflict of interest.

This article is a PNAS Direct Submission.

This open access article is distributed under Creative Commons Attribution-NonCommercial-NoDerivatives License 4.0 (CC BY-NC-ND).

Data deposition: The data reported in this paper have been deposited in the National Center for Biotechnology Information Sequence Read Archive database, <http://www.ncbi.nlm.nih.gov/sra> (accession no. SRP149887).

<sup>1</sup>A.-L.L. and A.L.R. contributed equally to this work.

<sup>2</sup>To whom correspondence should be addressed. Email: [research-charpentier@mpiib-berlin.mpg.de](mailto:research-charpentier@mpiib-berlin.mpg.de).

This article contains supporting information online at [www.pnas.org/lookup/suppl/doi:10.1073/pnas.1809663115/-DCSupplemental](http://www.pnas.org/lookup/suppl/doi:10.1073/pnas.1809663115/-DCSupplemental).

Published online October 31, 2018.

RNA abundance; and (iii) the ratio of WT and  $\Delta$ nase proportion of ends ensures that the transcript ends are detected as different between strains regardless of RNA abundance. Here, we improved this method for the in vivo genome-wide identification of transcripts targeted by the 3'-to-5' exoRNases YhaM, PNPase, and RNase R encoded in *S. pyogenes*.

## Results

In this study, we focused on the genome-wide identification and characterization of processing sites generated by three 3'-to-5' exoRNases: YhaM, PNPase, and RNase R. For this purpose, we compared the transcript 5' and 3' ends of WT and  $\Delta$ nase strains using triplicates of each dataset (*SI Appendix, Supplementary Materials and Methods*). We used parameters previously described by Le Rhun et al. (14) (i.e., thresholds for expression and proportion of ends in the WT and  $\Delta$ nase strains) and combined them with the statistical power of differential expression analysis using edgeR. The advantage of our approach is that it relies only on the ratio of the proportion of ends between WT and  $\Delta$ nase; therefore, the results are not affected by the abundance of the transcripts. The processing sites were detected when at least 2% of the transcripts were cleaved and the resulting fragments were stable in the cell.

We identified a total of 773, 1,438, and 82 transcript 5' and 3' ends varying between WT and  $\Delta$ SPy\_0267 (encoding YhaM and referred to as  $\Delta$ yhaM for convenience),  $\Delta$ pnpA, and  $\Delta$ rnr, respectively (Fig. 1A). Most of the affected transcript ends were 3' ends, which suggested that these enzymes have 3'-to-5' exoribonucleolytic activity in *S. pyogenes* (Fig. 1A). The 3' ends that are more abundant in the  $\Delta$ nase strain correspond to positions at which an RNase begins digesting and are referred to as "trimming start positions." Similarly, the 3' ends that are more abundant in the WT strain correspond to positions at which the RNase is blocked and are referred to as "trimming stop positions" (Fig. 1B). The distance between the trimming start position and the trimming stop position is the enzyme processivity (15).

**YhaM Trims the Majority of the Cell Transcript Ends Produced by Transcription Termination or EndoRNases.** By studying YhaM 3' ends, we retrieved 171 trimming start positions and 602 trimming stop positions (Fig. 1A and Dataset S1). On average, one processing site was detected per gene or intergenic region (*SI Appendix, Fig. S1A*). In addition, 112 of the 171 YhaM trimming start positions were located less than 10 nt downstream of trimming stop positions, with an average distance of 3 nt (Dataset S2). These data suggest that the *S. pyogenes* transcriptome is broadly targeted by YhaM and that YhaM has a low processivity (3 nt).

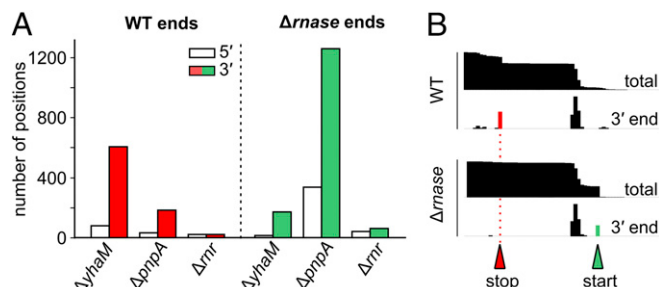


**Fig. 1.** Identification of 3'-to-5' exoRNase processing sites. (A) Number of transcript end positions more abundant in the WT (red) or in the  $\Delta$ nase (green). (B) Schematic representation of RNA sequencing profiling with annotated 3'-to-5' exoRNase trimming start (more abundant in the  $\Delta$ nase) and trimming stop (more abundant in the WT).

We examined the conserved sequence and the thermodynamic stability around the trimming start and stop positions and observed a stretch of uridines and increased stability of the RNA structure (decreased minimal free energy) upstream of the processing sites (*SI Appendix, Fig. S2*). Additionally, YhaM exhibited a strong preference for untranslated regions (UTRs) over ORFs (*SI Appendix, Fig. S1B*).

In agreement with these observations, half of YhaM processing sites were found within 10 nt downstream of predicted Rho independent transcriptional terminators or attenuators (Dataset S1). As the Rho protein is absent in *S. pyogenes* (16), throughout this paper, the term transcriptional terminator refers to Rho independent transcriptional terminators. The mean distance of the predicted terminator ends to the trimming start positions was 9 nt, and the mean distance of the predicted terminator ends to the trimming stop positions was 6 nt (*SI Appendix, Fig. S1C*). Accordingly, the conserved stretch of uridines was 3 nt closer to YhaM trimming stop positions than to the start positions (Fig. 2A and *SI Appendix, Fig. S2B*). In summary, the analysis of half of our data indicated that YhaM trims 3 nt, on average, from terminators and stops at the U stretch following their structure (Fig. 2B). We envisioned that the impact of YhaM on terminator processing (348 terminators targeted) was even broader than reflected in our results. Indeed, we recovered 3.5-fold more trimming stop positions than start positions, because trimming start positions located at the termination of transcription could not be recovered by our method (*SI Appendix, Fig. S3 A–C*).

The other half of YhaM processing sites, located in regions far from terminators, also showed the same sequence and structure conservation, although to a much lower extent, suggesting the presence of unpredicted terminators (Fig. 2C). Indeed, after manually removing 91 additional positions downstream of transcriptional attenuators or terminators, we did not find any clear sequence or structure conservation neighboring those sites, and we postulate that they resulted from YhaM trimming after endoRNase processing (*SI Appendix, Fig. S2D*). These remaining processing sites, representing 35% of all YhaM targets, were mostly found in ORFs (71%) (Dataset S1), therefore likely following processing by endoRNases. We detected the start and stop trimming positions in 42 transcripts (Dataset S2). Here again, the average and median processivity of YhaM was 3 nt. For example, we found that YhaM trimmed 1 nt of a few pre-tRNAs [trimming start and stop positions were detected for SPy\_t05 and SPy\_t46 (leucine), as well as for SPy\_t32 (histidine)]. This trimming was located at the 3' end presumably produced by endoRNase P during the 5' maturation of downstream tRNAs (17) (Dataset S2). We also retrieved YhaM processing sites in *secY* and *rplQ* transcript 3' UTRs, respectively 4 nt and 2 nt from the previously described endoRNase III cleavage sites (14). Thus, we show that, in addition to targeting terminators, YhaM targets transcript ends originating from RNase P and RNase III, and probably other endoRNases (Fig. 2D).

**YhaM ExoRNase Activity.** Our analysis indicates that at least 427 terminators were targeted by YhaM. With a total of 1,733 genes in the *S. pyogenes* genome and considering an average of two genes per operon (18), we estimated that more than 50% of all primary transcripts are targeted by YhaM. In addition, YhaM targeted transcript 3' ends after endoRNase processing. We validated the short processivity of YhaM by Northern blotting analyses comparing the size of 10 small transcripts in WT and  $\Delta$ yhaM (Fig. 2E and *SI Appendix, Fig. S4*) that were previously detected by small RNA (sRNA) sequencing (19). As expected from the RNA sequencing data, all of the detected transcripts were a few nucleotides shorter in the WT than in  $\Delta$ yhaM. A phylogenetic analysis of YhaM indicated that the protein from *S. pyogenes* is close to its orthologs from *B. subtilis* and *Staphylococcus aureus*, although it clustered slightly apart (*SI Appendix,*

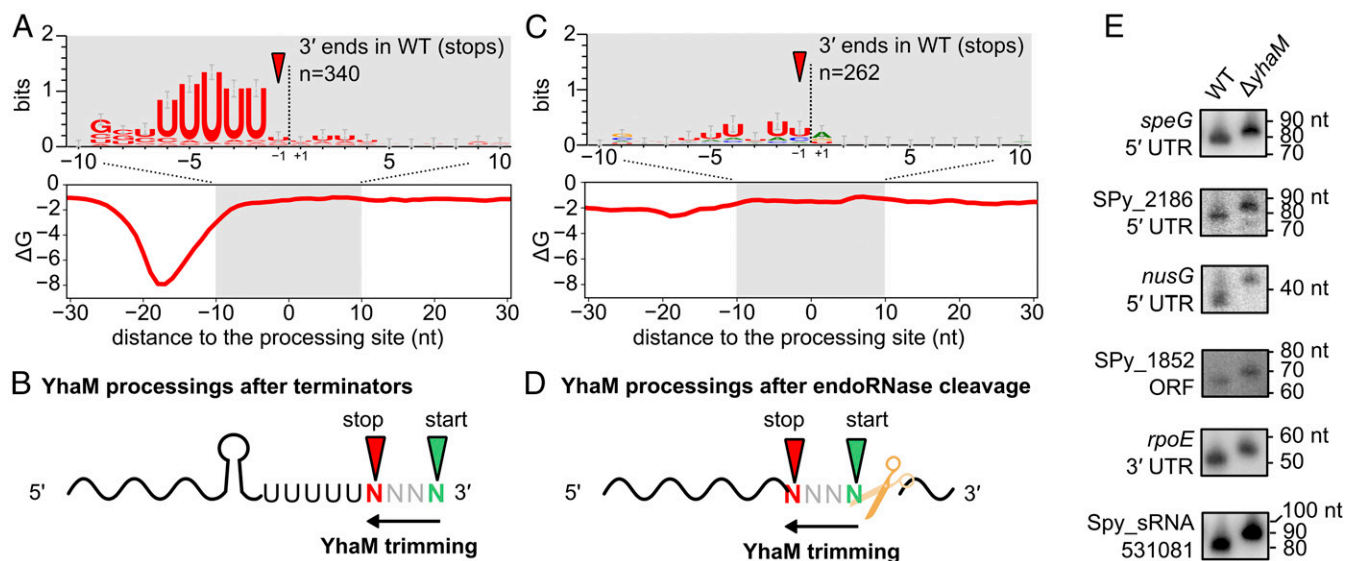


**Fig. 2.** YhaM trims a few nucleotides of transcript ends generated by transcription termination or endoRNase cleavages. The YhaM sequence logo is shown based on the sequence alignment of transcript 3' ends more abundant in WT compared with  $\Delta yhaM$ , located at either a maximal distance of 10 nt (A) or further from 10 nt (C) from predicted terminators. The average of the minimal free energy (25-nt length sequences) at each position surrounding YhaM processing sites (vertical dotted line) is shown. (B and D) Models for YhaM in vivo processing of transcript 3' ends. YhaM trims 3 nt, on average, of transcripts harboring intrinsic terminators (B) or generated from the processing by an endoRNase (scissors) (D). (E) Validation of YhaM short processivity in vivo by Northern blotting analyses in WT and  $\Delta yhaM$  (also *SI Appendix*, Fig. S4).

Fig. S5). Thus, it is possible that the global and unspecific ribonucleolytic activity that we observed is conserved in other bacterial genera.

**PNPase Is Involved in RNA Decay, Fully Degrading Short RNA Fragments.** We identified nearly sevenfold more 3'-end trimming start positions ( $n = 1,255$ ) than stop positions ( $n = 183$ ) for PNPase (Fig. 1A and *Dataset S1*). The fact that we detected the beginning of the trimming, but not the end, indicates that most targets are fully degraded by PNPase. If the trimming stop position corresponds to the transcriptional start site (TSS), it is not detected by our method (*SI Appendix*, Fig. S3 D and E). However, if PNPase degrades a complete RNA fragment whose 5' end is generated by an endoRNase (not a TSS), then this 5' end is retrieved by our method because it is present in  $\Delta pnpA$  and not in the WT. Indeed, we detected a larger amount of 5' ends more abundant in  $\Delta pnpA$  ( $n = 336$ ) than in WT compared with  $\Delta yhaM$  ( $n = 14$ ) or with  $\Delta mrn$  ( $n = 41$ ) (Fig. 1A). One hundred eighty-five of these 5' ends were located 50–200 nt upstream of 3'-end trimming start positions (*Dataset S4*). By extending our search from 200 to 1,000 nt for fragment length, only 32 additional putative fragments were detected. This suggested that short fragments (around 200 nt) generated by endonuclease cleavages are the major substrates of PNPase (Fig. 3A). In addition, by visual inspection of the data, we observed more RNA fragments that were not detected by our method because the PNPase trimming start or stop position matched with a terminator or a TSS, respectively (i.e., an end already abundant in the WT) (*SI Appendix*, Fig. S3 B and D). These fragments, also called decay intermediate fragments, are produced by endoRNases and are immediately degraded in the WT strain. PNPase indeed relies on endoRNases that initiate RNA decay, considering that more than 80% of the trimming start sites were located in ORFs (*SI Appendix*, Fig. S1B).

**PNPase Degrades Transcripts Consecutively to RNase III Processing.** We observed an overlap between PNPase trimming stop positions and the previously published double-strand-specific RNase III processing positions (14). The fact that some PNPase

trimming stop positions were not present in  $\Delta mrn$  indicated that PNPase trimmed those transcripts only after they were processed by RNase III. For instance, PNPase degraded several fragments resulting from the processing of 16S and 23S rRNA precursors by RNase III and other endoRNases (*SI Appendix*, Fig. S6), as well as *pnpA*, *rplQ* (50S ribosomal protein L17), and *nrdR* (transcriptional repressor of ribonucleotide reductase) (*SI Appendix*, Fig. S7 A–C).

In several bacteria, PNPase regulates its expression post-transcriptionally by degrading *pnpA* 5' UTR following RNase III processing in a stem loop (13). In *S. pyogenes*, nothing is known about the autoregulation of PNPase expression. Even though we cannot make conclusions about the biological impact of PNPase trimming on *pnpA* mRNA stability, we demonstrated that RNase III nicking activity produced a *pnpA* 5' UTR with two alternative 3' ends that were both targets of PNPase in vivo, as shown by RNA sequencing and Northern blotting analyses (*SI Appendix*, Fig. S7A).

**PNPase Targets Transcript 5' UTRs.** Several regulatory elements were targeted by PNPase, such as T-boxes and riboswitches. T-boxes are located in the 5' UTRs of aminoacyl-tRNA synthetase genes and regulate their expression by sensing charged or uncharged tRNAs, causing termination or antitermination, respectively. We observed an accumulation of decay intermediate fragments in  $\Delta pnpA$  compared with the WT for T-boxes, as well as for thiamine pyrophosphate, flavin mononucleotide (FMN), and glycine riboswitches (Fig. 3B and *SI Appendix*, Fig. S8A). For all regulatory 5' UTRs, we observed an accumulation of at least one decay intermediate fragment in  $\Delta pnpA$  by Northern blotting analyses (Figs. 3B and 4 and *SI Appendix*, Fig. S8A). The degradation fragments present only in  $\Delta pnpA$  were eventually degraded, either at a fast rate like the *trsA* T-box fragment or at slower rate like the *thrS* T-box fragment. This implies that one or several RNases substitute for PNPase activity, with different degrees of efficiency depending on the regulatory RNA targeted. In the case of FMN, the stability of the full-length regulatory RNA was increased in the PNPase deletion mutant (Fig. 3B and *SI Appendix*, Fig. S8B). It is therefore possible that PNPase

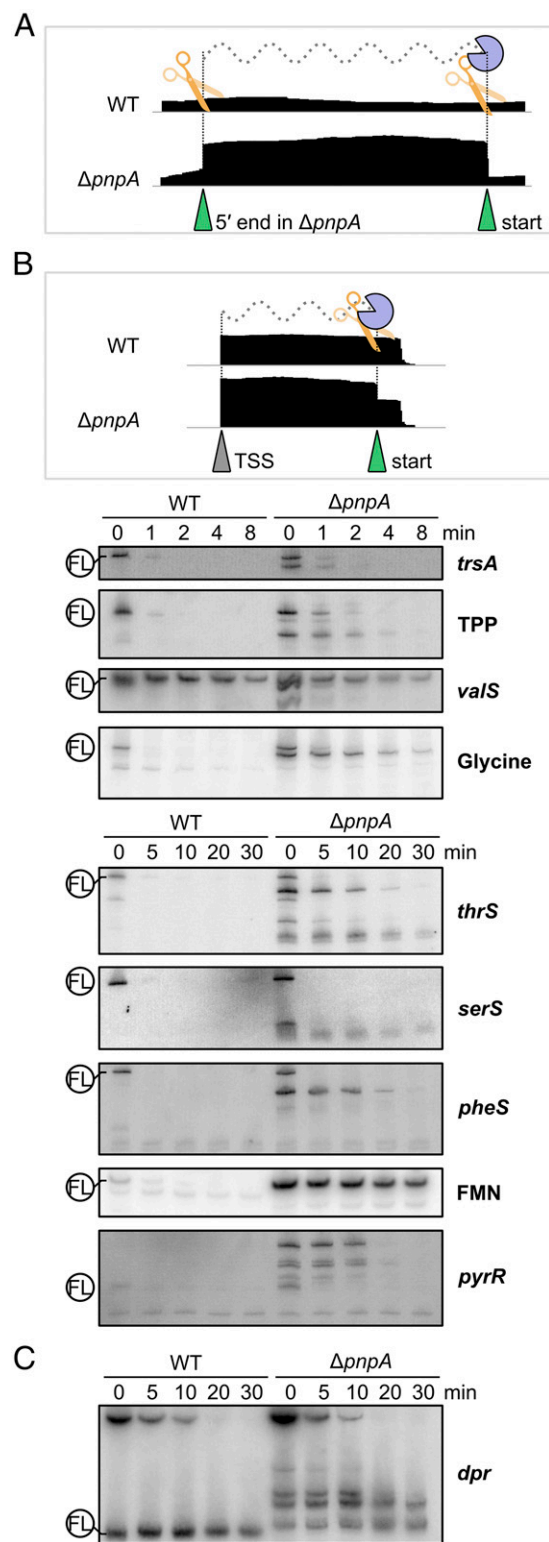


**Fig. 3.** PNPase degrades intermediate decay fragments. (A) Model for PNPase in vivo degradation activity. The intermediate decay fragments are generated by one or several endoRNases (scissors) and are fully degraded by PNPase (pacman) in the WT. (B) Model for in vivo PNPase degradation of 5' UTRs and Northern blotting analyses of T-boxes and putative riboswitches in WT and  $\Delta pnpA$ . An endoRNase (scissors) cleaves in the 5' UTR of the transcript, further degraded by PNPase (pacman) up to the TSS in the WT. (C) Northern blotting analysis of *dpr* 5' UTR in WT and  $\Delta pnpA$ . In B and C, RNA stability was investigated up to 8 or 30 min after addition of rifampicin to the medium to stop transcription (RNA sequencing coverage, loading

degrades this regulatory RNA in an endoRNase-independent fashion.

We also observed that PNPase trimmed the 5' UTR of *dpr*, which encodes a peroxide resistance protein protecting *S. pyogenes* from oxidative stress (20) (Fig. 3C and *SI Appendix, Fig. S84*). PNPase trimming stopped at one position but started at several positions. This indicated that either (i) the 5' UTR had multiple 3' ends (generated by transcription termination or endoRNases) that are targeted by PNPase or (ii) in absence of PNPase, another exoRNase substitutes to PNPase and processes this transcript, stalling at three different positions.

**RNase R Has Restricted Activity in *S. pyogenes* in Standard Growth Conditions.** We report 21 trimming stop positions and 61 trimming start positions for RNase R. We observed only two processing events, both of whose both start and stop positions were detected, and only six fragments accumulating in absence of the enzyme (*Datasets S2* and *S4*). One fragment of 69 nt was detected in 23S rRNAs, partially encompassing helix 42 and helices 43–44. This region of the 23S rRNA interacts with the ribosomal protein L11 and is part of the GTPase-associated center, which is responsible for binding GTPases during translation (21). By visual inspection, we observed another fragment originating from the *glyQ* T-box that was stabilized in absence of RNase R or PNPase (Fig. 4 and *SI Appendix, Fig. S8*). Therefore, both 3'-to-5' exoRNases degrade the *glyQ* T-box decay fragments, and RNase R seemed to be more efficient than PNPase in this degradation (Fig. 4).

**Deletion of 3'-to-5' ExoRNases Affects Bacterial Fitness at Cold Temperatures.** The growth of the single 3'-to-5' exoRNase deletion strains was comparable to the WT strain at 37 °C (*SI Appendix, Fig. S9A*). At 15 °C,  $\Delta rnr$  and  $\Delta yhaM$  presented a slower growth than the WT, with a more pronounced effect for the latter (*SI Appendix, Fig. S9B*). To investigate the importance of general 3'-to-5' exoribonucleic activity in *S. pyogenes*, we combined the exoRNase deletions. Whereas the  $\Delta pnpA$   $\Delta yhaM$  strain did not present any growth defect at 37 °C, the  $\Delta rnr$   $\Delta yhaM$  strain was slower to transition from exponential and stationary phases of growth (*SI Appendix, Fig. S9A*). The combined deletion of YhaM and RNase R at 15 °C exerted a synergic effect inhibiting the bacterial growth (*SI Appendix, Fig. S9B*), suggesting that both exoRNases have a distinct role in cold adaptation. We did not obtain the  $\Delta pnpA$   $\Delta rnr$  strain under the conditions tested, revealing that *S. pyogenes* needs at least PNPase or RNase R to be expressed.

## Discussion

In this study, we characterized the trimming positions of 3'-to-5' exoRNase genome-wide in *S. pyogenes*. We previously identified both 5' and 3' transcript ends produced by RNase III in *S. pyogenes* (14). Using our technique, we identified here the transcripts cleaved by YhaM, PNPase, and RNase R, three 3'-to-5' exoRNases expressed in *S. pyogenes* (22), and demonstrated their ribonucleolytic activity in this bacterium.

We would like to emphasize that we did not detect trimmings performed by several RNases stopping at the same position in this study (i.e., functional redundancy: one RNase substituting for the studied RNase), but only processing positions unique to the studied RNase. However, transcript 3' ends more abundant in  $\Delta rnr$ , presented here as positions where the trimming started, could correspond in some cases (e.g., when located

control, and half-life measurements are shown in *SI Appendix, Fig. S8*). Regulatory 5' UTR full lengths (FL) are indicated on the left side of the blots. TPP, thiamine pyrophosphate.

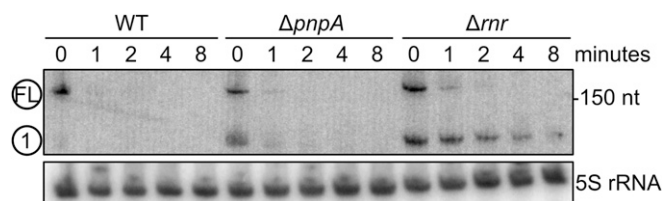


**Fig. 4.** *glyQ* T-box decay relies on RNase R and PNPase. RNA stability of the *glyQ* T-box was investigated in WT,  $\Delta pnpA$ , and  $\Delta mr$  up to 8 min after addition of rifampicin to the medium to stop transcription. The full-length (FL) T-box and the intermediate fragment of degradation (1) are indicated on the left side of the blot (half-life measurements are shown in *SI Appendix, Fig. S8B*).

upstream of the processing of the RNase of interest) to a substitute processing by another RNase.

We have demonstrated that YhaM targets the majority of the transcript ends (attributable to intrinsic terminators or endoRNases) in *S. pyogenes*. The apparent lack of specificity of this enzyme raises the question of its biological function. It was previously suggested that YhaM could protect the transcripts by trimming single-stranded RNA tails, thereby preventing the binding and further trimming by RNase R (4). However, we did not see a global decrease of RNA abundance in  $\Delta yhaM$  (*Dataset S3*), and we did not find conservation of strong structures that could protect the transcripts trimmed by YhaM (following endoRNase cleavage) from further degradation by exoRNases (*SI Appendix, Fig. S2*). As we observed that YhaM ribonucleolytic activity was not necessary for the mRNA fate, its function could be part of more general processes, such as replenishing the pool of nucleotides, similar to nanoRNases. Interestingly, YhaM overexpression partially rescued an *E. coli* strain conditionally deleted from OligoRNase (23). However, as opposed to nanoRNases, which degrade only very short RNA fragments (24, 25), YhaM targets and removes a few nucleotides of long transcripts. Finally, YhaM can also target DNA; indeed, *S. aureus* YhaM was originally identified as a DNA-binding protein enhancing plasmid replication (26), and *B. subtilis* YhaM was shown to degrade DNA in vitro (12, 23). It has been previously suggested that YhaM acts more as a DNase than an RNase in the cell (23, 27). Therefore, it is likely that *S. pyogenes* YhaM harbors DNA-binding or DNase capabilities in addition to the ribonucleolytic activity presented in this study.

Surprisingly, YhaM single- and double-deletion strains presented a strong phenotype at cold temperature (*SI Appendix, Fig. S9B*). YhaM does not seem to play a critical role in *S. pyogenes* RNA decay, and its global unspecific ribonucleolytic activity renders the identification of transcript targets that could explain this phenomenon difficult. It is possible that the DNA-binding and deoxyribonucleolytic activities play a role in this phenotype.

We have highlighted the low processivity of YhaM in vivo (3 nt trimmed, on average). It remains to be understood why this enzyme stalls after trimming a few nucleotides. The hypothesis that YhaM stops because of secondary structures is ruled out by the numerous trimming events of YhaM after endoRNase cleavage, where we did not detect any structure conservation (*SI Appendix, Fig. S2*). We propose the following hypotheses: (i) YhaM low processivity is an internal limitation (e.g., because of weak binding to the RNA); (ii) its very limited processivity could be explained if YhaM is a distributive enzyme (releasing its substrate after each nucleotide removed); or (iii) in vivo RNA processing by YhaM is blocked by RNA-binding factors (ribosomes, proteins, or RNA) or by a factor binding to YhaM. The fact that *B. subtilis* YhaM can process a 110-nt substrate in vitro without generating detectable intermediate fragments (12) could support the third hypothesis. A similar low processivity has been

recently mentioned for RNase II, which nibbled 2 nt, on average, downstream of terminators in *E. coli* but has not been further characterized (28). This peculiar short distance of trimming is therefore not exclusive to YhaM, and the purpose of this activity should be the focus of future investigations.

In agreement with the role of PNPase previously described in other bacteria, we observed that *S. pyogenes* PNPase is the main 3'-to-5' exoRNase degrading fragments generated by endoRNases during RNA decay (4, 29). Putative regulatory RNAs were also degraded by PNPase (*SI Appendix, Fig. S8A* and *Dataset S4*). In the case of regulatory RNA-binding molecules (i.e., riboswitches), it would be interesting to investigate if the degradation by PNPase is unspecific or directed toward the bound or unbound regulatory 5' subpopulation, as was described in *B. subtilis* (30, 31). In Gram-negative bacteria, PNPase was also shown to degrade sRNAs that are not associated with the RNA chaperone protein Hfq and to stabilize Hfq-bound sRNAs (32–34). *S. pyogenes* does not encode Hfq, and the absence of sRNAs stabilized by PNPase in this study is in agreement with those data.

Although the method that we used in this study does not allow detection of full transcript degradation (*SI Appendix, Fig. S3E*), the fact that very few genes were differentially expressed between WT and  $\Delta pnpA$  (*Dataset S3*) suggests that if PNPase also targets full transcripts, either this does not affect the transcript abundance or another RNase substitutes for PNPase in this function.

In *E. coli*, RNase R expression and activity are induced during stress conditions [e.g., upon cold shock (35)] in cells at the stationary phase of growth or in minimal medium (36). In *S. pyogenes*, the absolute amount of RNase R is lower than the amounts of PNPase and YhaM (37); therefore, similar mechanisms of regulation keeping RNase R levels low under standard conditions could explain the small targetome that we observed. Previous investigations about the role of RNase R in vivo have shown that this enzyme is important for the quality control and the stress-related degradation of ribosomes, for the degradation of faulty mRNAs as part of the *trans*-translation system, and for the degradation of highly structured mRNA fragments (38). The activity of RNase R in RNA decay was examined in *E. coli* and was observable only in absence of PNPase (8). Thus, a possible explanation for the limited number of RNase R targets and the absence of highly structured fragments accumulating in  $\Delta mr$  is that PNPase or another unknown 3'-to-5' exoRNase substitutes for RNase R activity in the deletion mutant. It is also possible that RNase R, due to its intrinsic helicase activity, favors the full degradation of transcripts (from the TSS to transcription termination position) that cannot be detected by our method (*SI Appendix, Fig. S2E*).

The single and double deletions of 3'-to-5' exoRNases did not have a strong impact on *S. pyogenes* growth at 37 °C (*SI Appendix, Fig. S9A*), and this result questions the role of 3'-to-5' exoRNases in RNA decay. Like many Gram-positive bacteria, *S. pyogenes* encodes for RNase J, which is the only bacterial RNase to exert 5'-to-3' exoRNase activity (39). The RNase J1 and J2 paralogs are the only known RNA decay-mediating RNases essential in *S. pyogenes*, suggesting that these enzymes and the 5'-to-3' exoRNase activity in general are key in this process (40). Interestingly, as we did not manage to mutate both *pnpA* and *mr* under the conditions tested, we hypothesize that *S. pyogenes* requires 3'-to-5' exoRNase activity. Even though the accumulation of fragments in  $\Delta pnpA$  indicates that none of the RNases present in *S. pyogenes* is able to substitute completely for PNPase, the expression of either PNPase or RNase R is sufficient for *S. pyogenes* survival. The relative importance of 3'-to-5' exoRNases versus 5'-to-3' exoRNases in the RNA decay pathway in *S. pyogenes* remains an open question.

In conclusion, YhaM has broad ribonucleolytic activity whose implication in biological processes requires further clarification. PNPase-mediated RNA decay in *S. pyogenes* follows the general model, whereby the degradation is triggered by an endonucleolytic cleavage. The role of RNase R is limited under standard culture conditions and needs to be investigated further.

## Materials and Methods

Bacterial cultures, construction of gene deletion mutants, RNA sequencing, read processing, differential transcript expression analysis, alignments of RNase cleavage site sequences and folding, plots, the phylogenetic tree, Northern blot assays, and quantifications were performed as described in *SI Appendix, Supplementary Materials and Methods*.

To find processing sites of RNases, we performed differential expression analysis on 5' and 3' read ends comparing the following datasets (triplicates): WT vs.  $\Delta yhaM$ , WT vs.  $\Delta rnr$ , and WT vs.  $\Delta pnpA$ . We prefiltered genome coverage data with a counts per million (cpm) value  $\geq 0.05$  in all six samples for each comparison (pairwise comparison of triplicates). Only 5'- or 3'-end positions with a cpm  $\geq 5$  in at least three samples were further processed. To account for compositional biases, end counts were normalized by trimmed mean of M-values normalization. Differentially expressed ends were then

defined using edgeR (v3.20.6) with an absolute log<sub>2</sub> fold change (FC)  $\geq 1$  and false discovery rate  $< 0.05$ . The parameters previously developed for specific cleavage position prediction (14) were applied to the results [i.e., proportion of ends of the reference strain  $\geq 2\%$  (WT strain when log<sub>2</sub> FC  $< 0$  and  $\Delta rnr$  strain when log<sub>2</sub> FC  $> 0$ ), ratio of proportion of ends (reference/mutant  $\geq 3$ )].

When at least two consecutive positions were identified in a window of 5 nt, the position with the highest proportion of ends value was chosen for further analyses. Gene expression values were calculated using the rpkm function from the edgeR package (41).

**ACKNOWLEDGMENTS.** We thank Richard Reinhardt and Bruno Huettel from the Max Planck Genome Centre Cologne for helpful discussion and for the sequencing of cDNA libraries preparation. We acknowledge Knut Finstermeier for RNA sequencing data analysis support. We thank Marc Erhardt for cohosting T.T.R. in his laboratory. We thank the members of the E.C. laboratory for discussions and critical reading of the manuscript. This work was funded by the Alexander von Humboldt (AvH) Foundation (AvH professorship to E.C.), the German Federal Ministry for Education and Research, the Max Planck Society, the Max Planck Foundation, the Swedish Research Council, and Umeå University. T.T.R. was supported by an AvH Foundation fellowship.

- Hui MP, Foley PL, Belasco JG (2014) Messenger RNA degradation in bacterial cells. *Annu Rev Genet* 48:537–559.
- Apirion D (1973) Degradation of RNA in *Escherichia coli*. A hypothesis. *Mol Gen Genet* 122:313–322.
- Andrade JM, Pobre V, Silva IJ, Domingues S, Arraiano CM (2009) The role of 3'-5' exoribonucleases in RNA degradation. *Prog Mol Biol Transl Sci* 85:187–229.
- Oussenko IA, Abe T, Ujiie H, Muto A, Bechhofer DH (2005) Participation of 3'-to-5' exoribonucleases in the turnover of *Bacillus subtilis* mRNA. *J Bacteriol* 187:2758–2767.
- Vincent HA, Deutscher MP (2006) Substrate recognition and catalysis by the exoribonuclease RNase R. *J Biol Chem* 281:29769–29775.
- Spickler C, Mackie GA (2000) Action of RNase II and polynucleotide phosphorylase against RNAs containing stem-loops of defined structure. *J Bacteriol* 182:2422–2427.
- Awano N, et al. (2010) *Escherichia coli* RNase R has dual activities, helicase and RNase. *J Bacteriol* 192:1344–1352.
- Cheng ZF, Deutscher MP (2005) An important role for RNase R in mRNA decay. *Mol Cell* 17:313–318.
- Huen J, et al. (2017) Structural insights into a unique dimeric DEAD-box helicase CshA that promotes RNA decay. *Structure* 25:469–481.
- Liou GG, Chang HY, Lin CS, Lin-Chao S (2002) DEAD box RhlB RNA helicase physically associates with exoribonuclease PNPase to degrade double-stranded RNA independent of the degradosome-assembling region of RNase E. *J Biol Chem* 277:41157–41162.
- Bonnin RA, Boulou P (2015) RNA degradation in *Staphylococcus aureus*: Diversity of ribonucleases and their impact. *Int J Genomics* 2015:395753.
- Oussenko IA, Sanchez R, Bechhofer DH (2002) *Bacillus subtilis* YhaM, a member of a new family of 3'-to-5' exonucleases in gram-positive bacteria. *J Bacteriol* 184:6250–6259.
- Briani F, Carzaniga T, Dehò G (2016) Regulation and functions of bacterial PNPase. *Wiley Interdiscip Rev RNA* 7:241–258.
- Le Rhun A, et al. (2017) Identification of endoribonuclease specific cleavage positions reveals novel targets of RNase III in *Streptococcus pyogenes*. *Nucleic Acids Res* 45:2329–2340.
- Fazal FM, Koslover DJ, Luisi BF, Block SM (2015) Direct observation of processive exoribonuclease motion using optical tweezers. *Proc Natl Acad Sci USA* 112:15101–15106.
- Washburn RS, Marra A, Bryant AP, Rosenberg M, Gentry DR (2001) Rho is not essential for viability or virulence in *Streptococcus aureus*. *Antimicrob Agents Chemother* 45:1099–1103.
- Frank DN, Pace NR (1998) Ribonuclease P: Unity and diversity in a tRNA processing ribozyme. *Annu Rev Biochem* 67:153–180.
- Taboada B, Ciria R, Martinez-Guerrero CE, Merino E (2012) ProOpDB: Prokaryotic Operon DataBase. *Nucleic Acids Res* 40:D627–D631.
- Le Rhun A, Beer YY, Reimegård J, Chylinski K, Charpentier E (2016) RNA sequencing uncovers antisense RNAs and novel small RNAs in *Streptococcus pyogenes*. *RNA Biol* 13:177–195.
- Tsou CC, et al. (2008) An iron-binding protein, Dpr, decreases hydrogen peroxide stress and protects *Streptococcus pyogenes* against multiple stresses. *Infect Immun* 76:4038–4045.
- Moazed D, Robertson JM, Noller HF (1988) Interaction of elongation factors EF-G and EF-Tu with a conserved loop in 23S RNA. *Nature* 334:362–364.
- Barnett TC, Bugrysheva JV, Scott JR (2007) Role of mRNA stability in growth phase regulation of gene expression in the group A streptococcus. *J Bacteriol* 189:1866–1873.
- Fang M, et al. (2009) Degradation of nanoRNA is performed by multiple redundant RNases in *Bacillus subtilis*. *Nucleic Acids Res* 37:5114–5125.
- Niyogi SK, Datta AK (1975) A novel oligoribonuclease of *Escherichia coli*. I. Isolation and properties. *J Biol Chem* 250:7307–7312.
- Mechold U, Fang G, Ngo S, Ogrzyzko V, Danchin A (2007) YtqI from *Bacillus subtilis* has both oligoribonuclease and pAp-phosphatase activity. *Nucleic Acids Res* 35:4552–4561.
- Zhang Q, Soares de Oliveira S, Colangeli R, Gennaro ML (1997) Binding of a novel host factor to the pT181 plasmid replication enhancer. *J Bacteriol* 179:684–688.
- Condon C, et al. (2008) Assay of *Bacillus subtilis* ribonucleases in vitro. *Methods Enzymol* 447:277–308.
- Lalanne JB, et al. (2018) Evolutionary convergence of pathway-specific enzyme expression stoichiometry. *Cell* 173:749–761.e38.
- Mohanty BK, Kushner SR (2003) Genomic analysis in *Escherichia coli* demonstrates differential roles for polynucleotide phosphorylase and RNase II in mRNA abundance and decay. *Mol Microbiol* 50:645–658.
- Deikus G, Babitzke P, Bechhofer DH (2004) Recycling of a regulatory protein by degradation of the RNA to which it binds. *Proc Natl Acad Sci USA* 101:2747–2751.
- Deikus G, Bechhofer DH (2009) *Bacillus subtilis* trp leader RNA: RNase J1 endonuclease cleavage specificity and PNPase processing. *J Biol Chem* 284:26394–26401.
- Andrade JM, Pobre V, Matos AM, Arraiano CM (2012) The crucial role of PNPase in the degradation of small RNAs that are not associated with Hfq. *RNA* 18:844–855.
- Bandyra KJ, Sinha D, Syrjanen J, Luisi BF, De Lay NR (2016) The ribonuclease polynucleotide phosphorylase can interact with small regulatory RNAs in both protective and degradative modes. *RNA* 22:360–372.
- Cameron TA, De Lay NR (2016) The phosphorolytic exoribonucleases polynucleotide phosphorylase and RNase PH stabilize sRNAs and facilitate regulation of their mRNA targets. *J Bacteriol* 198:3309–3317.
- Cairão F, Cruz A, Mori H, Arraiano CM (2003) Cold shock induction of RNase R and its role in the maturation of the quality control mediator SsrA/tmRNA. *Mol Microbiol* 50:1349–1360.
- Chen C, Deutscher MP (2010) RNase R is a highly unstable protein regulated by growth phase and stress. *RNA* 16:667–672.
- Wang M, Herrmann CJ, Simonovic M, Szklarczyk D, von Mering C (2015) Version 4.0 of PaxDb: Protein abundance data, integrated across model organisms, tissues, and cell-lines. *Proteomics* 15:3163–3168.
- Domingues S, et al. (2015) The role of RNase R in trans-translation and ribosomal quality control. *Biochimie* 114:113–118.
- Laalami S, Putzer H (2011) mRNA degradation and maturation in prokaryotes: The global players. *Biomol Concepts* 2:491–506.
- Bugrysheva JV, Scott JR (2010) The ribonucleases J1 and J2 are essential for growth and have independent roles in mRNA decay in *Streptococcus pyogenes*. *Mol Microbiol* 75:731–743.
- Robinson MD, McCarthy DJ, Smyth GK (2010) edgeR: A bioconductor package for differential expression analysis of digital gene expression data. *Bioinformatics* 26:139–140.